Separation of Sensor Control and Data in Closed-Loop Sensor Networks

Victoria Manfredi*, Jim Kurose*, Naceur Malouch†, Chun Zhang‡ and Michael Zink*
*Dept. Computer Science, University of Massachusetts, Amherst, MA 01003 USA
† University Pierre et Marie Curie, LIP6, 8, Rue du Capitaine Scott, 75015 Paris - FRANCE
‡ IBM T.J. Watson Research Center, Hawthorne, NY 10532 USA

***Abstract*—Sensor networks are prone to congestion due to bursty and high-bandwidth data traffic, combined with wireless links and many-to-one data routing to a sink. Delayed and dropped packets then degrade the performance of the sensing application. In this paper, we investigate the value of separate handling of sensor control and data traffic, during times of congestion, in a closed-loop sensor network. We first show that prioritizing sensor control traffic over data traffic decreases the round-trip control-loop delay, and consequently increases the quantity and quality of the data collected by the sensor network. We then ground our analysis in a closed-loop meteorological sensor network, focusing on a storm-tracking application running over a network of X-band radars. Our application measures reflectivity (a measure of the number of scatterers in a unit volume of atmosphere known as a voxel) and tracks storms (i.e., regions of high reflectivity) using a Kalman filter. Considering data quantity, we show that prioritizing sensor control traffic increases the number of voxels, V, that can be scanned given a constant number of reflectivity samples, N_c, obtained per voxel. Here, utility increases linearly with the number of scanned voxels. Considering data quality, we show that prioritizing sensor control traffic increases the number of reflectivity samples, N, that can be obtained per voxel given a constant number of voxels, V_c, to scan. Here, since sensing accuracy improves only as a function of $\sqrt{N}$, the gain in accuracy for the reflectivity estimate per voxel as N increases is relatively *small* except when prioritizing sensor control increases N significantly (such as when sensor control packets suffer severe delays). Because accuracy also degrades as a function of $\sqrt{N}$, however, and because prioritizing sensor control traffic reduces the number of control packets dropped, data degradation is mitigated. Considering the performance of the tracking application, we then show that during times of severe congestion, not prioritizing sensor control can actually lead to tracking errors accumulating over time.**

I. Introduction

Sensor networks are prone to congestion due to bursty and high-bandwidth data traffic, combined with wireless links and many-to-one data routing to a sink [1], [2]. Delayed and dropped packets then degrade the performance of the sensing application. In a *closed-loop sensor network* (i.e., a sensor network where sensors send data to a control center and sensor controls flow back to the sensors), the sensed data transmitted through the network may have considerable redundancy in both time and space making application performance somewhat insensitive to data packet loss and delay. Conversely, performance is typically much more sensitive to loss or delay of sensor control packets, since these packets carry the application's sensor commands generated in response to received data. Consequently, there are potential advantages to separate handling of sensor control and data traffic.

In this paper, we investigate the value of separate handling of sensor control and data traffic, during times of congestion, in a closed-loop sensor network. We first show that prioritizing sensor control traffic over data traffic decreases the round-trip control-loop delay, and consequently increases the quantity and quality of the data collected by the sensor network. We then ground our analysis in a closed-loop meteorological sensor network [3]–[5], focusing on a storm-tracking application running over a network of X-band radars. The storm-tracking application measures reflectivity in the atmosphere and tracks storms (i.e., regions of high reflectivity) using a Kalman filter as in [6]; reflectivity is a measure of the number of scatterers in a unit volume of atmosphere known as a voxel. The reflectivity data are transmitted from the radars over a shared wireline [3], [4] or wireless [5] network to a control center that periodically generates radar targeting (sensor control) commands based on features detected in the data.

To evaluate the utility of separate handling of sensor control and data traffic in our storm-tracking application, we compare the performance of aggregate FIFO for both sensor control and radar data packets with that of priority forwarding of sensor control packets. Considering data quantity, we show that prioritizing sensor control traffic increases the number of voxels, V, that can be scanned given a constant number of reflectivity samples, N_c, obtained per voxel. Here, utility increases linearly with the number of scanned voxels. Considering data quality, we show that prioritizing sensor control traffic increases the number of reflectivity samples, N, that can be obtained per voxel given a constant number of voxels, V_c, to scan. Here, since sensing accuracy improves only as a function of $\sqrt{N}$, the gain in accuracy for the reflectivity estimate per voxel as N increases is relatively *small* except when prioritizing sensor control increases N significantly (such as when sensor control packets suffer severe delays). Because accuracy also degrades as a function of $\sqrt{N}$, however, and because prioritizing sensor control traffic reduces the number of control packets dropped (so sensors execute "correct" rather than default sensor controls), data degradation is mitigated. Considering the performance of the tracking application, we show that during times of severe congestion, not prioritizing sensor control traffic over data traffic can actually lead to tracking errors accumulating over time.

In one sense, our results mirror those in [7] regarding differential traffic handling and network-based (rather than sensor-application-based) performance metrics: "that performance is generally satisfactory in a classical best effort network as long as link load is not too close to 100%," and that "there appears little scope for service differentiation beyond the two broad categories of 'good enough' and 'too bad.'" *However, unlike some other network applications, the sensing application can still perform well during times of severe congestion, when sensor control packets are given priority, because (i) sensor controls are not dropped, so sensors execute "correct" rather than default sensor controls, and (ii) sensing accuracy both improves and degrades slowly in the number of sensed data samples obtained.*

While previous work [8]–[12] focuses on prioritizing network control packets, our focus here is on prioritizing sensor control packets. Whereas network control affects what data are transmitted and at what rate, sensor control additionally affects what data are actually sensed and thus available to be transmitted. Consider object tracking and suppose that the sensor controller incorrectly asks to sense data from one location in the environment when the object is at a different location. The data that should have been collected from sensing the different location cannot be collected retroactively, as the environmental conditions may have changed (i.e., the object may have moved) during the time that the incorrect location was sensed. Thus, in a closed-loop sensor network, the issue is not just that data may be received late, but that the opportunity to ever sense some data may be missed completely. Other work in sensor networks has considered service differentiation [13]–[15], including during times of congestion [16], but does not specifically look at the effects of prioritizing sensor control nor consider closed-loop sensor networks.

The remainder of this paper is structured as follows. In Section II, we overview related work. In Section III, we discuss general characteristics of a closed-loop sensor network. In Section IV, we describe our meteorological sensing application. In Section V, we present simulation results comparing the performance of FIFO with that of priority forwarding of sensor control packets. Section VI concludes this paper.

II. Related Work

The notion of separate handling of control and data packets in a network has a long history. The SS7 signaling system [8] that carries control packets in telephone networks is a packet-switched control network that is physically separate from the circuit-switched network carrying voice traffic. In ATM networks, Q2931 signaling packets for virtual circuit management are carried over connections that are logically separated from data traffic [9]. For IP networks, it is possible for operators to configure routers to provide prioritized service for "control" protocols such as BGP or SNMP. In wireless networks, [12] advocates for a separate control channel for controlling access to a shared medium. Proposals for priority handling of TCP acknowledgments [10], [11] can also be considered as providing a different level of service to control packets (ACKs) than data packets. While this previous work focuses on prioritizing network control packets, our focus here is on prioritizing sensor control packets.

Other work, in sensor networks, has considered service differentiation for different classes of traffic. [13] assigns priority levels to packets, forwarding higher-priority packets more frequently over more paths to achieve higher probability of delivery. [14] allocates rates to flows based on the class of traffic being sent and the estimated load on the network. [15] considers bandwidth reservation for high-priority flows in wireless sensor networks. [16] proposes congestion-aware routing in sensor networks, providing differential service to high priority data traffic versus low-priority data traffic in congested areas of the network. None of these approaches, however, considers the effects of prioritizing only sensor control in a closed-loop sensor network.

Control theory considers the effects of a network within the control loop in the field of "Networked Control Systems" [17]. As in a closed-loop sensor network, data and sensor control are sent over a network. Unlike in a closed-loop sensor network, however, the sensor control and data packets in a Networked Control System are constrained to be the feedback (sensor control) and measurements (data) of a classical control system. Consequently, the ratio of data to control is much smaller than that of a closed-loop sensor network such as our radar network [3], [4]. Since any data packet (i.e., measurement) in a Networked Control System may now be as important as any sensor control packet (i.e., feedback), it is not necessarily beneficial to always give higher priority to sensor control. Instead, packets are scheduled to optimize expected performance using the control equations, for instance by incorporating the error incurred due to network delays directly into the control equations [18], or by optimally dropping selected data measurements during times of overload by analyzing the effect of the resulting missing measurements on the control equations [19]. Networked Control Systems can thus be considered a specific sub-class of the more general closed-loop sensor networks we consider in this work.

III. Closed-Loop Sensor Networks

A generic closed-loop sensor network is shown in Figure 1: data are streamed from sensors to a control center, while sensor commands flow from the control center back to the sensors. The control center closes the system's main control loop by ingesting data, computing statistics from the data, and selecting each sensor's future data collection strategy based on the statistics. As shown in Figure 2, a closed-loop sensor network periodically computes a new sensor control. At the start of the kth update interval, t_k, the control center issues a command to the sensor specifying how to collect data. After a delay of β_k, the command is received at the sensor. The sensor then begins transmitting back measured data; α_k is the delay of data from the sensor to the control center before the kth control update interval. After time Δ, the sense-and-response cycle then repeats. We assume that the duration, Δ, of each

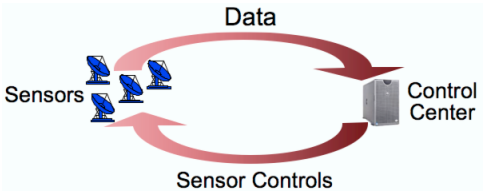

Fig. 1. A closed-loop sensor network.

control update interval is fixed, but that the length of Δ could also depend on time or another metric.

From Figure 2, the sensor control computed at time t_k is based on data that the sensor sent by time $t_k - \alpha_k$. The sensor control is then applied at the sensor at time $c_k = t_k + \beta_k$. When computing sensor control c_{k+1}, we assume that it is preferable to use only the most recent data, obtained with sensor control c_k. Thus, while data obtained under sensor control c_{k-1} could continue to be transmitted by the radars during time d_{k-1} to time c_k, and could additionally be used to compute sensor control c_{k+1}, this data is now out-of-date, and we assume that it is not transmitted. While not considered here, such out-of-date data could also be sent as low priority background traffic.

Suppose now that packets are delayed: then the α_k and β_k delays will increase and the total amount of data from control c_k received by time t_{k+1} at the control center will decrease. Since the ratio of data to sensor control traffic is large, it should be possible to provide significantly better performance to sensor control traffic (e.g., lower end-to-end delays and lower loss) with only a minimal performance degradation of the data traffic, as illustrated in Figure 2(b) and in keeping with queueing theoretic conservation laws [20]. This then decreases the "round trip" delay for the control loop - the summed delay of sensed data from a sensor to the control center and the delay of sensor control packets back to the sensor. Lower round-trip delays enable the control center to examine more data before making a control decision, resulting in more accurate estimates of the sensed quantity of interest, which should then give better application-level performance. Consequently, prioritizing sensor control in a closed-loop sensor network should give both *more data* and *better quality data*. We explore these two benefits in more detail below.

A. More Data

One use of the additional data obtained by prioritizing sensor control is to allow sensing of more environmental locations. In a meteorological sensing network, sensing more environmental locations translates to the radar sensing more voxels. Equivalently, in a camera network [21] comprised of pan-tilt-zoom cameras, sensing more environmental locations translates to the camera collecting images from more different locations in the environment. In both the radar and camera networks, this additional data increases the probability that an object of interest (storm, person, car, etc.) is detected. From p. 35 of [22] "the data processing inequality can be used to show that no clever manipulation of the data can improve the

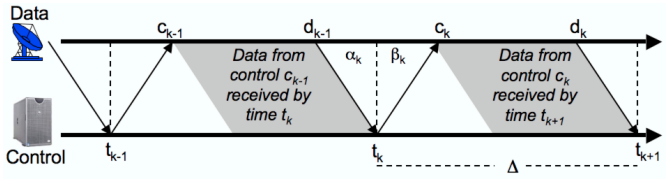

(a) $\alpha_k \approx \beta_k$

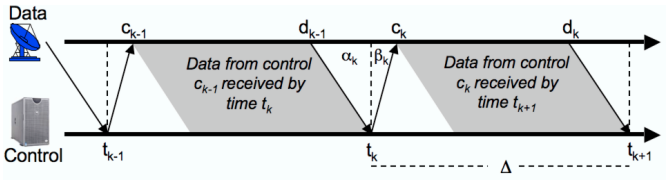

(b) $\alpha_k > \beta_k$

Fig. 2. Timing of the control loop when (a) $\alpha_k \approx \beta_k$ and (b) $\alpha_k > \beta_k$.

inferences that can be made from the data." Consequently, we expect the utility gain from additional data to be at most a linear function of the amount of additional data obtained.

To quantify the amount of additional data obtained when prioritizing sensor control, consider the effect of the length of the control update interval Δ. For FIFO scheduling, data are collected during a time interval of length $\Delta - \alpha_k - \beta_k$, while for priority scheduling, data are collected during a time interval of at most length $\Delta - \alpha_k$. Consequently, priority scheduling has a percentage gain of at most $\beta_k/(\Delta - \alpha_k - \beta_k)$ more time over FIFO. As Δ decreases, the percentage gains from priority scheduling thus increase. As Δ increases, although the total amount of data that is collected will increase, the gains from priority scheduling will decrease.

B. Better Quality Data

Another use of the additional data obtained by prioritizing sensor control is to improve data quality. In a meteorological sensing network, more data samples from the same environmental location translates to more reflectivity samples per voxel, thereby decreasing the standard deviation of the reflectivity estimate for the voxel, see Section IV-B. Equivalently, in an acoustic sensor network, more signals from the same environmental location can be used to perform signal averaging to reduce noise [23], while in a camera sensor network, more images from the same environmental location can be used to perform image averaging to reduce noise [24].

To quantify the gain in data quality when prioritizing sensor control, consider the number of i.i.d. data samples $X_1, \ldots, X_n$ collected during time $t = \Delta - \alpha_k - \beta_k$. Increasing t linearly increases the number of samples n collected. Suppose, however, that we use those samples to compute an unbiased estimator $W(\mathbf{X})$ of some parameter θ (such as reflectivity or temperature). The Cramer-Rao bound [25] says that the standard deviation of $W(\mathbf{X})$ from θ, $\mathrm{SD}_\theta(W(\mathbf{X}))$, can be lower bounded as follows,

$$\mathrm{SD}_\theta(W(\mathbf{X})) \geq \frac{1}{\sqrt{n\mathcal{I}}} \qquad (1)$$

where $\mathcal{I}$ is the Fisher information, representing the information a sample contains about the estimator $W(\mathbf{X})$. As $\mathrm{SD}_\theta(W(\mathbf{X}))$ decreases only at the rate of $1/\sqrt{n}$, sensing accuracy improves slowly in the number of sensed data values obtained. For our meteorological radar network (and for acoustic [23] and camera [24] sensor networks), the reflectivity (or noise) standard deviation when averaging over n i.i.d data samples decreases as a function of $\sqrt{n}$.

Even during times of packet loss, not just packet delays, prioritizing sensor control improves data quality. Consider an overloaded network in which packets may be dropped. Since prioritizing sensor control limits the number of sensor control packets dropped, suppose that only data packets are dropped. As the number of i.i.d. data samples, n, decreases, the standard deviation of any estimator increases only at the rate of $1/\sqrt{n}$. Thus, sensing accuracy both improves *and* degrades slowly in the number of data samples. Additionally, because sensor control packets are not dropped, sensors are able to execute the "correct" sensor controls (instead of executing a default control such as having a radar scan 360° or a camera take low-quality images of all environment locations), thereby obtaining even better quality data, Consequently, the sensing application may still perform well during times of network overload, if data packets, but not sensor control packets, are dropped.

IV. Meteorological Application

In this section, we describe the networked meteorological remote sensing application we use to illustrate and quantitatively explore the effect of prioritizing sensor control on data quantity and quality, and on application-level performance. As in Figure 1, remote X-band radars transmit measured reflectivity values to a control center. The Meteorological Command and Control (MC&C) [4] component at this control center identifies meteorological features from the radar data, reports the features to end-users, and determines each radar's future scan strategy (i.e., the volume of the atmosphere to be scanned by each radar). A 4-node system has been developed and deployed in southwestern Oklahoma as part of the CASA project [26]. As in Figure 2, the system operates on a Δ=30-second control update interval. We now describe our network and radar meteorology models, and the storm-tracking application running over the network.

A. Network Model

In this section, we describe how we model the effect of prioritizing sensor control on the data delay, α_k, and sensor control delay, β_k, during congestion, as well as how we model packet drops. To model packet delays, we assume a wireless network where data is sent from radars (sources) to a control center (the sink), and sensor control commands are sent back to the radars from the control center. We analyze the packet delays incurred at a bottleneck link, assuming other network delays are small enough to be ignored. In a wireless sensor network, the bottleneck link might be the last hop node before the sink. We consider two scheduling mechanisms: *(1)* aggregate FIFO service of sensor control and data packets and *(2)* nonpreemptive priority forwarding of sensor control packets. For instance, when using 802.11, priority forwarding over the wireless links could be done as in [27] by assigning queuing, waiting, and back-off times based on priority level.

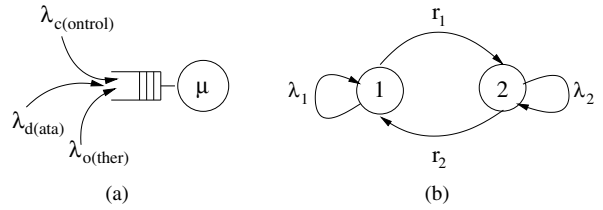

Fig. 3. (a) Model of the bottleneck queue in the network. (b) The 2-state Markov modulated Poisson process used to model the "other" traffic.

Figure 3(a) shows our queue model of the bottleneck link. We group traffic contending for the bottleneck queue into three flows: sensor *control* traffic destined for some node r, *data* traffic generated by node r, and *other* traffic including data and sensor control traffic either generated by or destined for nodes other than node r. Although data and sensor control packets might always travel in opposite directions in a sensor network, due to the wireless links, data and sensor control packets will still compete against each other for access to the wireless link; consequently, we model the bottleneck link as a single queue. For wired links, data and sensor control packets may end up in the same outgoing queue when there are, e.g., (i) multiple control centers, (ii) multiple sensor applications using the same network, or (iii) asymmetric routing.

Since data and sensor control are generated at deterministic intervals in the CASA network, we assume that sensor control and data packets have deterministic arrivals with rates λ_c and λ_d respectively. "Other" packets arrive according to a two-state Markov-modulated poisson process, see Figure 3(b), where packets arrive on average at rate λ_o; in state 1 packets arrive at rate λ_1, in state 2 packets arrive at rate λ_2, and transitions from states 1 to 2 and from states 2 to 1 occur at rates r_1 and r_2 respectively. To vary the burstiness, as measured using the index of dispersion, see [28], we vary the values of λ_1 and λ_2 while keeping λ_o constant. Finally, we assume that the packet service time is exponentially distributed with rate μ. To compute the delays through the bottleneck queue, we use the ns-2 simulator [29], see Section V.

To model packet drops, e.g., due to overload, we compare the worst-case and best-case scenarios. For the worst-case scenario, we assume that all sensor control packets are dropped and that the default sensor control must be used. For the best case scenario, we assume that no sensor control packets are dropped and that the scan strategy specified by the sensor controls always collect data that is optimal for the application performance metrics defined in the next section.

B. Radar Meteorology Model

In this section, we describe the radar meteorology model we use to evaluate the effect of prioritizing sensor control on application performance. A radar operates by sending out pulses at a given rate as it sweeps through the sector it is

scanning. For a given time duration, the smaller the sector scanned, to some minimum sector size, the better the estimated reflectivity values, since the radar can send more pulses per volume of atmosphere, see [30]. Meteorological algorithms use reflectivity values to identify, e.g., storms and tornados. We now describe the application performance metrics of interest.

1) Number of Voxels Scanned: Suppose that the number of pulses, N_c, transmitted per voxel is fixed, where a voxel is a unit volume of atmosphere. Then the simplest metric of interest is the number of voxels, V, that can be scanned during time $\Delta - \alpha_k - \beta_k$, given by,

$$V = \frac{(\Delta - \alpha_k - \beta_k) f_p}{N_c} \quad (2)$$

where $f_p = 3$ kHz is the pulse repetition frequency. We ignore here how the voxels are distributed to form a sector scan. As $\Delta - \alpha_k - \beta_k$ increases, the number of voxels V that can be scanned, each with N_c pulses, increases linearly.

2) Reflectivity Standard Deviation: We now relax the assumption that the number of pulses transmitted per voxel is constant. We focus here on the quality of the reflectivity metric estimated from the data. The number of pulses, N, transmitted per voxel given a constant number of voxels, V_c, and during a time interval of length $\Delta - \alpha_k - \beta_k$ is [30],

$$N = \frac{(\Delta - \alpha_k - \beta_k)\, f_p}{V_c} \quad (3)$$

where $f_p = 3$ kHz is the pulse repetition frequency, $V_c = \frac{\delta\theta\, \delta\phi}{\theta\, \phi}$, $\delta\theta$ is the size of the sector scanned in degrees, see Figure 4, $\theta = 1.8°$ is the antenna beamwidth, $\delta\phi = 12°$ is the elevation height, and $\phi = 2°$ is the elevation step (i.e., the increase in elevation after a horizontal scan). Following Equation 3, as the sector size $\delta\theta$ decreases, more pulses can be transmitted per voxel.

Each pulse transmitted per voxel returns an estimate of the reflectivity for that voxel. Reflectivity is a measure of the number of scatterers in a volume of atmosphere. Averaging over more samples increases the confidence in the estimated reflectivity value. Given N samples for a voxel, the reflectivity standard deviation, $\hat{\sigma}_r$, for the voxel is [30]:

$$\hat{\sigma}_r = 1 + \sqrt{\frac{1}{N}\left(\left(1 + \frac{1}{S_n}\right)^2 + \left(\frac{1}{S_n}\right)^2\right)} \quad (4)$$

where S_n is the signal to noise ratio and has a typical value of 10dB. Computing $\sigma_r = 10\log_{10}(\hat{\sigma}_r)$, we obtain the reflectivity standard deviation in decibels (dB). While increasing $\Delta - \alpha_k - \beta_k$ linearly increases the number of samples N collected, the standard deviation of the estimated reflectivity value of the voxel decreases only at the rate of $1/\sqrt{N}$, exemplifying the Cramer-Rao result seen in Section IV.

3) Root mean-squared error (RMSE) when tracking a storm: Both the number of voxels scanned and the reflectivity standard deviation evaluate system performance only within a single control update interval, Δ. To capture whether per-interval gains accumulate across multiple intervals, we look to simulations tracking a storm (i.e., a region of high reflectivity). We first discuss how we convert the standard deviation of reflectivity to the standard deviation of the location of peak reflectivity (i.e., the location of the storm centroid). We then describe how the standard deviation of the location of the storm centroid affects the RMSE when tracking the centroid.

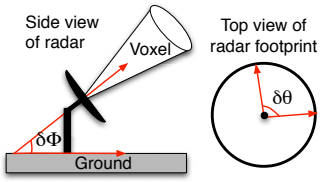

Fig. 4. Radar definitions.

The reflectivity standard deviation, σ_r, depends, through N in Equation (3), on the scan sector size, $\delta\theta$, and the time spent scanning the sector, $\Delta - \alpha_k - \beta_k$. An increase in σ_r should translate into an increase in the standard deviation of the location of the peak reflectivity, σ_z. As there are many algorithms for detecting peak reflectivity, and the uncertainty associated with the location depends on the algorithm, we adopt a simple approach here and set the value of σ_z along a radial from the radar as,

$$\sigma_z = \frac{\sigma_r D_r}{30dB} \quad (5)$$

where D_r is the distance of the object from the radar and 30dB is a mid-range reflectivity value. This assumes that uncertainty in the reflectivity estimate translates into an equivalent amount of uncertainty in the location of peak reflectivity.

We use the standard deviation in the location of peak reflectivity in the covariance matrix of the Kalman filter used to track storms, described in the next section. For meteorological algorithms, it is not sufficient to scan only the storm centroid. Instead, reflectivity data from the surrounding area (i.e., the entire storm cell) is also needed [4]. Hence our experiments will perform tracking based on the location of the storm centroid, but will also scan the surrounding area, corresponding to the expected storm radius.

C. Storm-Tracking Application

In this section we describe a storm-tracking application. Let $\mathbf{x}_k$ be the true location of the storm centroid at time k and let $\mathbf{y}_k$ be noisy measurements of the location. A Kalman filter [31] assumes that the true location at time k is a linear function of the true location at time $k-1$ plus Gaussian noise, and that the noisy measurements at time k are a linear function of the true location at time k plus Gaussian noise. I.e.,

$$\mathbf{x}_k = \mathbf{A}\mathbf{x}_{k-1} + N[\mathbf{0}, \mathbf{Q}_k] \quad (6)$$

$$\mathbf{y}_k = \mathbf{C}\mathbf{x}_k + N[\mathbf{0}, \mathbf{R}_k] \quad (7)$$

We now describe our Kalman filter model of the movement of a storm centroid. We use $\mathbf{x}_k = [x^1, x^2, x^3, x^4]$, where x^1 is the true x-location of the storm centroid, x^2 is the true y-location,

x^3 is the true x-velocity, and x^4 is the true y-velocity. For the noisy measurements, we use $\mathbf{y}_k = [y^1, y^2]$, where y^1 is the measured x-location and y^2 is the measured y-location. Then,

$$\mathbf{A} = \begin{bmatrix} 1 & 0 & \Delta & 0 \\ 0 & 1 & 0 & \Delta \\ 0 & 0 & 1 & 0 \\ 0 & 0 & 0 & 1 \end{bmatrix}, \ \mathbf{C} = \begin{bmatrix} 1 & 0 & 0 & 0 \\ 0 & 1 & 0 & 0 \end{bmatrix}$$

$$\mathbf{Q} = \begin{bmatrix} 0 & 0 & 0 & 0 \\ 0 & 0 & 0 & 0 \\ 0 & 0 & q^3 & 0 \\ 0 & 0 & 0 & q^4 \end{bmatrix}, \ \mathbf{R}_k = \begin{bmatrix} r^1 & 0 \\ 0 & r^2 \end{bmatrix}_k$$

We obtain the covariance matrix $\mathbf{Q}$ as follows. First, we assume that the latitude and longitude noises are uncorrelated and set the off-diagonal elements of $\mathbf{Q}$ to zero. We also assume that there is no noise in the latitude and longitude locations. We then compute the noise in the latitude and longitude velocities from 39 existing storm tracks from the National Severe Storms Laboratory courtesy of Kurt Hondl and the WDSS-II software [32]. Each track is a series of $(latitude, longitude)$ coordinates. We first compute the differences in latitude and longitude, and in time, between successive pairs of points. We then fit the differences using Gaussian distributions. Since the length of a latitude degree at 40° latitude equals 111.04 km and the length of a longitude degree at 40° latitude equals 85.39 km, we obtain, in units of km/hour, that the latitude velocity is $\sim N(9.1, 1268)$ and that the longitude velocity is $\sim N(16.7, 836)$. For example, the latitude velocity is on average 9.0 km/hr with one standard deviation of $\sqrt{1268} = 35.6$ km/hr. Working in seconds, we set $q^3 = 0.0001$ and $q^4 = 0.00006$. While the process noise $\mathbf{Q}$ is not a function of time k, the measurement noise $\mathbf{R}_k$ is, as it depends both on the radar scan strategy at time k, and on the delay given by $\alpha_k + \beta_k$. Thus, at time k, we compute σ_z as in Equation (5) and set $r^1 = r^2 = \sigma_z^2$.

We use the Kalman filter parameters just described in the tracking algorithm used in Section V. As the system is not directly observable, it can be difficult to exactly obtain the covariance matrices in practice. Consequently, to parameterize the Kalman filter used to generate the trajectory of the storm centroid, we use the same parameters as the Kalman filter used for tracking, but we perturb the covariance matrices as follows.

$$\mathbf{Q} = \begin{bmatrix} 1 & 0 & 0 & 0 \\ 0 & 1 & 0 & 0 \\ 0 & 0 & q^3 & 0 \\ 0 & 0 & 0 & q^4 \end{bmatrix}, \ \mathbf{R}_k = \begin{bmatrix} 5r^1 & 0 \\ 0 & 5r^2 \end{bmatrix}_k$$

We now describe the storm-tracking application. Assume that the radar is located at the origin, that the radar radius is 40km (e.g., as with the CASA radars [4]), and that the radar stops tracking a storm when it exits the radar's footprint. We represent a storm as a circle with a 3km radius based on work by [33] on storm cells which gives 2.83km as "the radius from the cell center within which the intensity is greater than e^{-1} of the cell center intensity"; the initial location of the storm centroid is chosen randomly and subsequent movement is governed by Equation 6. To compute the measured location of the storm centroid, $\mathbf{y}_k$, we use Equation 7, using $\Delta - \alpha_k - \beta_k$ and the procedure described earlier to obtain the parameters for the covariance matrix $\mathbf{R}_k$. To compute the estimated true location $\hat{\mathbf{x}}_k$ from $\mathbf{y}_k$, and to compute the predicted true location $\hat{\mathbf{x}}^-_{k+1}$ and covariance matrix $\mathbf{P}^-_{k+1}$, we use the filtering equations, e.g., see [31]. To compute the area that contains $\hat{\mathbf{x}}^-_{k+1}$ with 99% confidence, we use its covariance matrix $\mathbf{P}^-_{k+1}$. The 99% confidence area is an ellipse centered at the point $(\hat{x}^1_{k+1}, \hat{x}^2_{k+1})$ whose semi-axes are given by the submatrix $\mathbf{P}^-_{k+1}[1, 2; 1, 2]$. $\hat{x}^1_{k+1}$ and $\hat{x}^2_{k+1}$ are, respectively, the x- and y-locations of the storm centroid and are the first two components of the vector $\hat{\mathbf{x}}_{k+1}$. To account for the storm radius, we expand the confidence ellipse by 3km (since the ellipse gives the area in which the storm centroid will be found 99% of the time, but does not include the storm radius). We compute the radar's next scan sector to be the smallest scan angle that covers the expanded confidence ellipse. The radar then scans this sector for $\Delta - \alpha_{k+1} - \beta_{k+1}$ seconds during the next update interval; the radar scans 360° initially, whenever the true location lies outside of the scanned area, and when $\alpha_k + \beta_k \geq \Delta$.

V. Simulation Results

In this section, we use the models described in Section IV to investigate the value of prioritizing sensor control over data in our illustrative closed-loop meteorological sensing network. We first examine the effect of prioritizing sensor control on data quantity and quality, and then examine the effect on tracking-application performance.

A. Simulation Set-up

1) Delayed Packets: To obtain the control-loop delays we use the ns-2 simulator [29]. We set the queue size to be large enough that no packets are dropped. The data delay is the delay incurred by the last packet that is processed at the bottleneck node by the start of each update interval. The corresponding control delay is the delay of the associated sensor control packet for that update interval. Based on experimental results from the CASA radar testbed, we use $\frac{\lambda_c}{\lambda_c + \lambda_d} = 0.0005$ and $\Delta = 30$ sec, setting $\lambda_c = \frac{1}{30}$ pkts/sec and $\lambda_d = \frac{2000}{30}$ pkts/sec. We also use $\Delta = \{5, 15\}$ sec, setting $\lambda_c = \frac{1}{\Delta}$ pkts/sec while leaving λ_d unchanged; such Δs are feasible for a phased array radar [34]. For the "other" traffic, we set $\lambda_o = \frac{2000}{30}$ pkts/sec, with $\lambda_1 = p\lambda_o$ and $\lambda_2 = (1-p)\lambda_o$, for $p = \{0.5, 0.2, 0.05\}$. We set the transition rates r_1 and r_2 for the Markov modulated Poisson process to each be 1.0 sec on average. Computing the index of dispersion (idx), see [28],

$$idx \quad = \quad 1 + \frac{2(\lambda_1 - \lambda_2)^2 r_1 r_2}{(r_1 + r_2)^2(\lambda_1 r_2 + \lambda_2 r_1)} \qquad (8)$$

shows that our parameters consider $idx \approx \{1, 25, 55\}$. $idx = 1$ corresponds to a Poisson process while larger values correspond to increased traffic burstiness. Finally, since $\lambda_c + \lambda_d + \lambda_o \approx 133.37$ pkts/sec we set $\mu = 148.5$ pkts/sec achieving a load of about 0.90. Even with $\frac{(\lambda_c + \lambda_d + \lambda_o)}{\mu} < 1$, however, the bursty "other" traffic introduces temporary overload conditions. Using this network model, for each parameter setting,

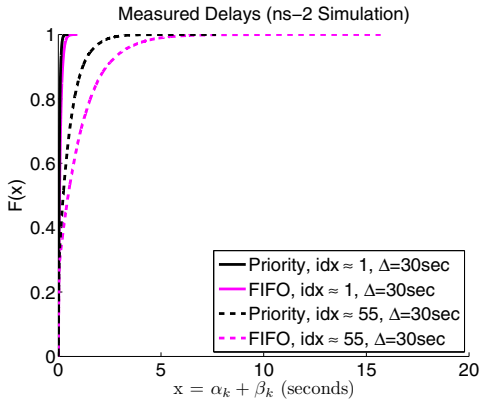

(a)

Fig. 5. CDFs of the measured $\alpha_k + \beta_k$ delays.

we perform 10 simulation runs, of 100,000 sec each. This gives, for instance, 20,000 update intervals per run for $\Delta = 5$ sec. For each run we obtain a time-varying series of $\alpha_k + \beta_k$ delays. Figure 5 shows the delay distributions for $\Delta = 30$ sec; we plot the data from all runs to obtain the CDF for each scheduling mechanism and idx pair. Although not shown, we also find that on average, the $\alpha_k + \beta_k$ delay for priority scheduling is about half that of FIFO, regardless of Δ (we observe a maximum average delay of ~ 0.9 sec for FIFO with $\Delta = 5$ sec and $idx = 55$). While we expect that increasing λ_o will increase the $\alpha_k + \beta_k$ delays, recall from Section III that prioritizing sensor control has a percentage gain of at most $\beta_k/(\Delta - \alpha_k - \beta_k)$ more time over FIFO. Consequently the relative performance gain of priority over FIFO should be bounded regardless of λ_o.

2) Dropped Packets: To model packet drops only, we compare the worst-case (all sensor control dropped) and best-case (no sensor control dropped) scenarios. We assume that the sensor control packets always tell the radar to scan 45° and two elevation angles within that sector (i.e., the smallest sector that would be scanned by the CASA radars, and correspondingly, the highest quality data that would be obtained). Consequently N_{45} samples per voxel would be collected in the specified 45° sector. As a result of overload, we assume that a fraction p_{loss} of packets are lost. For both FIFO and priority scheduling, a fraction of the data samples will be lost. Additionally for FIFO, however, since we assume the worst case, all sensor control packets will be lost, and the radars will always use the default strategy of scanning 360° and all six elevation angles (i.e., the largest volume of space that the CASA radars would scan), collecting N_{360} samples per voxel.

B. Data Quantity and Quality

Effect of Packet Delays on Number of Voxels Scanned: Plugging the delays generated from ns-2 into Equation 2, Figure 6(a) shows the number of times more voxels scanned under priority scheduling than under FIFO. Figure 6(a) shows that as Δ decreases and burstiness increases, the benefits of prioritizing increase: for $\Delta = 5$ sec and $idx = 55$, priority

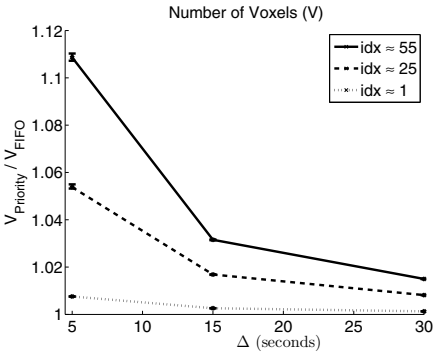

(a)

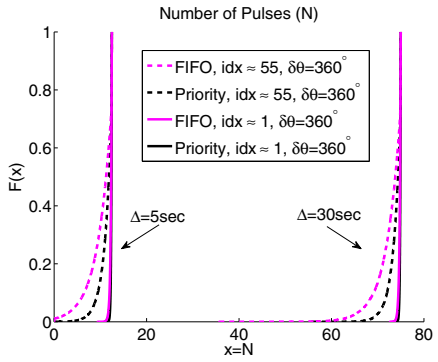

(b)

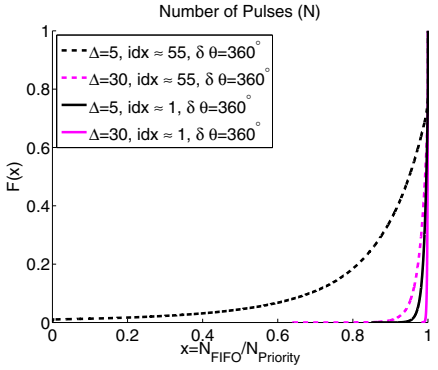

(c)

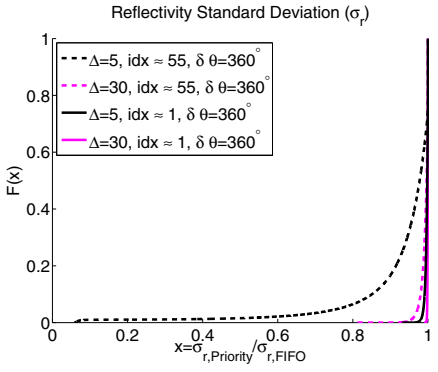

(d)

Fig. 6. (a) Number of times more voxels V scanned under priority scheduling than under FIFO; 95% bootstrap confidence intervals over 10 simulation runs are shown. (b) CDFs of the number of pulses, N. (c) CDFs of the normalized number of pulses. (d) CDFs of the normalized reflectivity standard deviation.

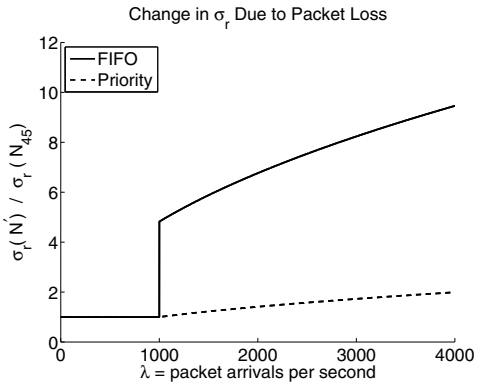

Fig. 7. Packet loss under different arrival rates. Capacity is 1000 pkts/sec.

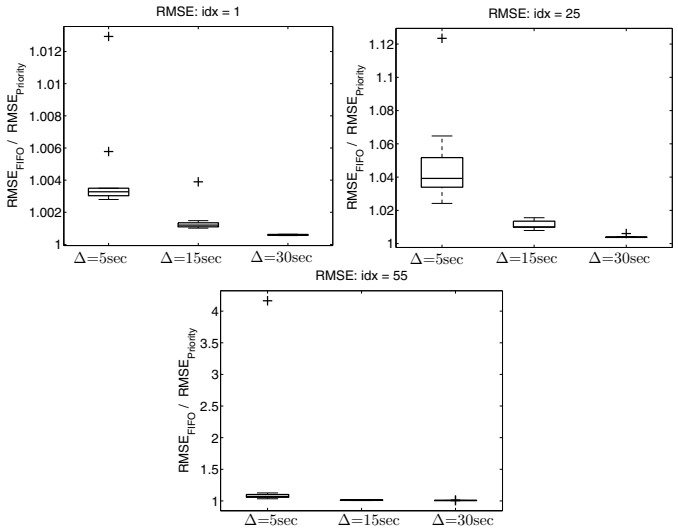

Fig. 8. RMSE from tracking application. Boxplots are over 10 runs. Boxes show the median and first and third quartiles; +'s indicate outliers, i.e., data values more than 1.5 times greater (smaller) than the third (first) quartile.

scheduling scans about 1.15 times as many voxels as FIFO.

Effect of Packet Delays on Reflectivity Standard Deviation: Plugging the delays generated from ns-2 into Equation 3, for $\delta\theta = 360°$ we obtain a time-varying series of Ns. The empirical CDFs for N are shown in Figure 6(b), using the data from all 10 runs for each CDF: we see that FIFO and priority each achieve about $6\times$ as many pulses for $\Delta = 30$ sec as for $\Delta = 5$ sec and that the total number of pulses gained over FIFO from using priority is independent of Δ. Figure 6(c) plots the ratio of each FIFO CDF in Figure 6(b) with that of the corresponding priority CDF. Figure 6(c) shows that for $idx = 1$ or $\Delta = 30$ sec, FIFO achieves at least 90% as many pulses as priority, more than 95% of the time. Only for $idx = 55$ and $\Delta = 5$ sec (very bursty traffic and a small update interval), does FIFO perform significantly worse (achieving $\sim 80\%$ as many pulses as priority $\sim 80\%$ of the time).

Plugging the time-varying series of Ns into Equation 4, we obtain the corresponding series of reflectivity standard deviation σ_r values. Figure 6(d) plots the ratio of each priority σ_r CDF with that of the corresponding FIFO σ_r CDF, again using the data from all runs. Due to the $1/\sqrt{N}$ behavior in Equation 4, Figure 6(d) shows that the gains in N from prioritizing sensor control are diminished: e.g., now for $idx = 55$ and $\Delta = 5$ sec, priority scheduling has at least 90% as much uncertainty as FIFO about 90% of the time. To summarize, Figures 5 and 6 show while the $\alpha_k + \beta_k$ delays for priority scheduling are about half of those for FIFO, these gains do not translate into equivalent $\%$ gains in N or σ_r, and the gains are greater for smaller Δs and more overloaded links.

Effect of Packet Drops on Reflectivity Standard Deviation: From our simulation setup for dropped packets, FIFO will have $N' = N_{360} \times (1 - p_{loss})$ data samples per scanned voxel reach the control center while priority will have $N' = N_{45} \times (1 - p_{loss})$ data samples per scanned voxel reach the control center. From [30] we use $N_{360} = 750$ and $N_{45} = N_{360} \times 3 \times 8 = 18000$. Figure 7 plots the reflectivity standard deviation when N' samples reach the control center (i.e., there is loss), normalized by the reflectivity standard deviation when N_{45} samples reach the control center (i.e., there is no loss). We assume that the network delivers packets at its capacity and that traffic beyond network capacity is lost. Hence, $N' = N_{45}$ for both FIFO and priority when arrivals are less than capacity; when arrivals exceed capacity, $N' = N_{360} \times (1 - p_{loss})$ for FIFO and $N' = N_{45} \times (1 - p_{loss})$ for priority. Figure 7 shows that as the system goes into overload, σ_r degrades gracefully for priority scheduling, as the offered load increases (i.e., the fraction of lost data samples increases). These results show that by prioritizing sensor control, the sensing system is robust to network overload conditions, and suggest that in times of congestion, it is preferable for the end-to-end data transfer protocol to ignore lost data samples, rather than adopting an ARQ protocol for retransmission, that would then increase the data delays to RTT timescales.

C. Performance of Storm-Tracking Application

Effect of Packet Delays on Tracking Error: We plug the delays generated from ns-2 into the tracking application in Section IV-D. At each control update we compute the next scan sector. Figure 8 shows the RMSE under FIFO relative to that of priority. The RMSE is computed over the differences between the true, $\mathbf{x}_k$, and estimated true, $\hat{\mathbf{x}}_k$, locations of the storm centroid. As Δ decreases and burstiness increases, Figure 8 shows that the benefits of prioritizing increase: for $\Delta = 5$ sec and $idx = 55$, FIFO has a median of about 1.06 times the RMSE of priority scheduling. We also see some outliers: e.g., for $\Delta = 5$ sec and $idx = 55$, when FIFO has about 4.17 times the RMSE of priority. For this outlier run, the average scan angle was about $56°$ while for the other 9 runs, the average scan angle ranged from $36°$ to $46°$. Hence, once the scan angle (and consequently the measurement noise) is sufficiently large, the Kalman filter less effectively filters out the noise when estimating the true location. As it is not possible by prioritizing sensor control to gain even 4x more data (let alone 4x better reflectivity standard deviation) within a single update interval, then at least some of the outliers are

due to errors accumulating over multiple intervals. Thus, for tracking, it is possible for per-interval performance gains or losses to accumulate across multiple update intervals, unlike with the voxel and reflectivity standard deviation metrics.

VI. Conclusions

In this paper, we examined the value of prioritizing sensor control traffic over data traffic in closed-loop sensor networks. Our results show that during times of network congestion, prioritizing sensor control gives more data, better quality data, and better application-level performance than does FIFO scheduling of both sensor control and data packets. There are several directions for future work. It would be interesting to see whether other sensor network applications, besides tracking, have performance metrics for which gains can accumulate across multiple decision epochs. While this work assumed that each sensed value is equally valuable, in practice, sensed data from areas of interest, such as areas of high reflectivity in the meteorological application, are likely to be more important to a sensing application, e.g., see [35]. These data values could be handled at higher priority, while other data values could be transmitted at lower priority or discarded in times of congestion. The more general challenge is to define an overall architecture for pushing application-level performance considerations down into the lower layers of the system stack in an application-independent manner.

Acknowledgments

The authors thank Brian Donovan and David McLaughlin for enlightening discussions about radar meteorology, and Bruno Ribeiro for comments on a paper draft. This research was supported in part by the National Science Foundation, award number NSF CNS-0519998, by the National Science Foundation under the Engineering Research Centers Program, award number EEC-0313747, and via an International Research in Engineering Education supplement to award number EEC-0313747. Any opinions, findings and conclusions or recommendations expressed in this material are those of the authors and do not necessarily reflect those of the National Science Foundation.

References

[1] B. Hull, K. Jamieson, and H. Balakrishnan, "Mitigating congestion in wireless sensor networks," in *SenSys*, 2004.

[2] C.-Y. Wan, S. Eisenman, A. Campbel, and J. Crowcroft, "Siphon: Overload traffic management using multi-radio virtual sinks in sensor networks," in *SenSys*, 2005.

[3] D. McLaughlin, V. Chandrasekar, K. Droegemeier, S. Frasier, J. Kurose, F. Junyent, B. Philips, S. Cruz-Pol, and J. Colom, "Distributed collaborative adaptive sensing (DCAS) for improved detection, understanding, and predicting of atmospheric hazards," in *Proc. American Meteorological Society Annual Meeting*, 2005.

[4] M. Zink, E. Lyons, D. Westbrook, J. Kurose, and D. Pepyne, "Closed-loop architecture for distributed collaborative adaptive sensing of the atmosphere: Meteorological command and control," *International Journal of Sensor Networks*, to appear.

[5] B. Donovan, A. Hopf, J. M. Trabal, B. J. Roberts, D. J. McLaughlin, and J. Kurose, "Off-the-grid radar networks for quantitative precipitation estimation," in *Proc. European Radar Conference*, 2006.

[6] V. Manfredi and J. Kurose, "Scan strategies for adaptive meteorological radars," in *Advances in Neural Information Processing Systems 21*, 2007.

[7] S. B. Fredj, T. Bonald, A. Proutiere, G. Regnie, and J. Roberts, "Statistical bandwidth sharing: A study of congestion at flow level," in *Proc. ACM Sigcomm*, August 2001.

[8] I. E. Consortium, "Signaling system 7 (ss7)," *http://www.iec.org/online/tutorials/ss7/*, 2006.

[9] U. Black, *ATM: Foundation for Broadband Networks*. Prentice Hall, 1995.

[10] L. Kalampoukas, A. Varma, and K. Ramakrishnan, "Improving TCP throughput over two-way asymmetric links: Analysis and solutions," in *Proc. ACM Sigmetrics*, 1998, pp. 78–89.

[11] H. Balakrishnan, V. Padmanaban, G. Fairhurst, and M. Sooritabandara, "TCP performance implications of network path asymmetry," *Request for Comment, RFC 3449*, Dec. 2002.

[12] P. Kyasanur, J. Padhye, and V. Bahl, "On the efficacy of separating control and data into different frequency bands," in *Proc. Broadnets*, 2005.

[13] S. Bhatnagar, B. Deb, and B. Nath, "Service differentiation in sensor networks," in *Fourth International Symposium on Wireless Personal Multimedia Communications*, 2001.

[14] K. Karenos, V. Kalogeraki, and S. V. Krishnamurthy, "A rate control framework for supporting multiple classes of traffic in sensor networks," in *26th IEEE International Real-Time Systems Symposium*, 2005.

[15] W. L. Tan, O. Yue, and W. C. Lau, "Performance evaluation of differentiated services mechanisms over wireless sensor networks," in *Vehicular Technology Conference*, 2006.

[16] R. Kumar, R. Crepaldi, H. Rowaihy, A. F. H. III, G. Cao, M. Zorzi, and T. F. L. Porta, "Mitigating performance degradation in congested sensor networks," *IEEE Transactions on Mobile Computing*, vol. 7:6, 2008.

[17] P. F. Hokayem and C. T. Abdallah, "Inherent issues in networked control systems: A survey," in *Proc. American Control Conference*, 2004.

[18] G. C. Walsh and H. Ye, "Scheduling of networked control systems," *IEEE Control Systems Magazine*, 2001.

[19] M. Lemmon, Q. Ling, and Y. Sun, "Overload management in sensor-actuator networks used for spatially-distributed control systems," in *SenSys*, 2003.

[20] L. Kleinrock, *Queueing Systems Volume II*. Wiley Interscience, 1976.

[21] I. Akyildiz, T. Melodia, and K. Chowdhury, "A survey on wireless multimedia sensor networks," *Computer Networks*, vol. 51, 2007.

[22] T. Cover and J. Thomas, *Elements of Information Theory*. Wiley Interscience, 2006.

[23] A. D'Costa and A. Sayeed, "Data versus decision fusion for classification in sensor networks," in *International Conference of Information fusion*, 2003.

[24] J. Boyce, "Noise reduction of image sequences using adaptive motion compensated frame averaging," in *ICASSP*, 1992.

[25] G. Casella and R. Berger, *Statistical Inference*, 2002.

[26] Center for Collaborative Adaptive Sensing of the Atmosphere, "http://www.casa.umass.edu," 2006.

[27] X. Pallot and L. Miller, "Implementing message priority policies over and 802.11 based mobile ad hoc network," in *Milcom*, 2001.

[28] H. Heffes and D. Lucantoni, "A markov modulated characterization of packetized voice and data traffic and related statistical multiplexer performance," *IEEE Journal on Selected Areas in Communication*, vol. 4:6, 1986.

[29] "The network simulator ns-2," in *http://www.isi.edu/nsnam*.

[30] B. Donovan and D. J. McLaughlin, "Improved radar sensitivity through limited sector scanning: The DCAS approach," in *Proc. AMS Radar Meteorology*, 2005.

[31] G. Welch and G. Bishop, "An introduction to the Kalman filter," U of North Carolina at Chapel Hill, Dept. of Computer Science, Tech. Rep. TR95-041, 1995.

[32] K. Hondl, "Capabilities and components of the warning decision and support system - integrated information (WDSS-II)," in *Proc. American Meteorological Society Annual Meeting*, 2003.

[33] I. Rodrigues-Iturbe and P. Eagleson, "Mathematical models of rainstorm events in space and time," *Water Resources Research*, vol. 23:1, pp. 181–190, 1987.

[34] M. Sanchez-Barbetty and R. Jackson, "Architecture for low cost electronically steered phased arrays," in *IEEE MTT International Microwave Symposium*, 2008.

[35] M. Li, T. Yan, D. Ganesan, E. Lyons, P. Shenoy, A. Venkataramani, and M. Zink, "Multi-user data sharing in radar sensor networks," in *SenSys*, 2007.